Information Sciences and Computer Engineering, Vol. 1, No. 1, (2010) 26–36

PHARUS

International Journal of
Information Sciences and Computer Engineering

journal homepage: http://www.ijisce.org

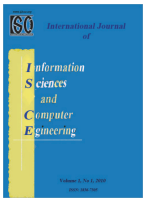

Nonlinear Control of PWM Multilevel Inverter-Fed Induction Motors

Lazhar Manaï[a,*], Faouzi Ben Ammar[a,b]

[a] *INSAT Centre Urbain Nord: Centre LP N°676 1080 Tunis*
[b] *L.S.E: Laboratory of the Electric Systems, ENIT LP 37-1002 Tunis the belvedere, Tunisia*

***Abstract*– This paper presents a method to design a new control algorithm, using the nonlinear feedback transformation technique to deal with the control problem of multilevel inverter-induction motors system. To provide effective control, nonlinearities and flying capacities voltages variations in the model must be taken into account in the control design. Based on input-output linearization theory, a decoupled nonlinear control strategy is obtained for induction motor by assuring multilevel inverter capacities voltages stabilization. Simulation results demonstrate that the approach proposed in this paper is correct, and the control strategy designed is effective.**

Keyword: Feedback linearization, multilevel inverter-induction motor modelling, nonlinear systems, nonlinear control.

1. Introduction

Along with the development of power electronics and microelectronics, nonlinear systems and control theory have witnessed tremendous development. Feedback linearization is one of the most active research areas. It considered as a powerful tool for control of nonlinear systems and it has been successfully applied to the control of power electronics based systems [1, 2]. In view of the non linear multivariable and strongly coupling characteristics of AC machines some researchers use the newly developed feed back linearization to realize decoupling control [3]. In feedback linearization the nonlinear induction motor modeling is transformed to a linear one by choosing a different state representation [4]. An equivalent linear model of the original one is obtained by using nonlinear transformation [5].

Recently, multilevel inverters have appeared as a new breed of power inverters to feed induction motor. The main advantages of these inverters include the increase of power, the reduction of voltage stress on power switching devices and the generation of high quality output voltages. Multilevel inverters have drawn a tremendous attention and have been studied for several high-voltages and high-power (rolling mill, traction...) since they have particular advantages that suit these types of applications [6]. In this paper, the modelling of the multilevel inverter fed induction machine shows the existence of various types of non linearities. These non linearities are caused at first in the state matrix, by the strong coupling between induction motor variables states, in particular between the flux and the torque, on the second part by the non linearities in the control matrix caused by the dependence between the flying capacitor voltage sources, the stator current and the control signal of adjacent cells of multilevel inverter. In thus conditions, the stabilization of the flying capacities voltages is undoubtedly one of the most important problems. In literature, several proposals in high-voltage high-power treat induction motor and multilevel inverter as a separately system to resolve nonlinearities, under certain conditions a simple open-loop control guarantees natural balancing of the flying voltages [7, 8, 9, 10]. For example if the impedance of the load is high at the switching frequency, the dynamic of natural balancing is very low, consequently an extra hardware "balance booster" RLC filter is introduced between multilevel inverter and the induction machine [11, 12, 13]. In order to control the non-linear system without "balance booster" it is necessary to make use of non linear control techniques. The Algorithm control law proposed by authors consists to decouple rotor flux and angular speed by assuring multilevel inverter flying capacities voltages stabilization.

The remainder of this paper is organized as follows. We give in section 2 a brief review of multilevel inverter topologies and the control strategies, in Section 3, we develop the four level inverter output voltages expressions. In Section 4, the fort dependence between multilevel inverter capacities voltages and stator current evolution is proved based on an analysis of the current in each capacity for various power switches states. In Section 5, we develop the modelling system by taking into account the flying capacities voltages variations. Section 6 shows how the developed algorithm provides rotor flux and angular speed decoupling in one hand and multilevel inverter capacities voltages stabilization on the other hand. Finally, simulation results are presented in Section 7 with some brief concluding remarks.

2. Review of Multilevel Inverter Topologies and Control Strategies

In high voltage high power conversion system, the blocking voltage capability of the power switch semiconductors gives a

*Correspondence author:
Email address: manaii_lazhar@yahoo.fr, Ph: +216 71 703829

limitation on the maximal allowed DC link voltage for the conventional bipolar inverter. In the other hand, the limitation of the switching frequency for the high power switches increases difficulties in building PWM inverter with a wide output frequency range. It is therefore of significant practical importance to increase the number of levels in the output voltage with a harmonic voltage spectrum, which is outside the pass band characteristics of the load. The technology of the series connection of large turn-off devices is very difficult because of the dispersion of turn-off time from one device to another [11]. This problem is resolved by connecting in series several controllable cells based on a single device connection to get multilevel topology like: the diode clamped multilevel inverter (NPC) [11, 12, 13], the Flying Capacitor Multilevel Inverter (FCMI) also called imbricated cells multilevel inverter [11, 14, 15] shown by figure1and represents the topology considered in this paper, the Cascaded Multilevel Topology and the Hybrid Multilevel Topology [16, 17].

The PWM modulation of the multilevel inverter must in the same time permit the balance of the number of switching transitions between the cells and preserve the natural balancing property of this inverter. Different modulation strategies are used to optimized the spectral quality of this inverter, like the Phase Shifted Carriers PWM (PSCPWM) [11], the Phase Disposition PWM (PDPWM) and the Centered Space Vector PWM (CSVPWM) [17, 18].

The conventional modulation approach strategy control adopted in this paper is the Phase Shifted Carriers PWM (PSCPWM) since it satisfies to the principal objectives of the multilevel inverter. As shown in figure 2, for the PSCPWM control the cell switching is controlled by a sine-triangle comparison, every cell possess its carrier waveform and a common reference sine waveform. For an N level inverter (with p commutation cells), per phase the PSCPWM uses ($p = N - 1$) carrier waveforms of the same amplitude, frequency and phase-shift $\alpha = \frac{2\pi}{p}$ between the adjoining cells and each carrier is compared with three-phase sine waveform variable frequency.

3. Four Level Inverter Output Voltages Expressions

Each phase of the four level inverter shown by figure1, is composed of 3 commutations cells connected with a set of two flying-capacitor voltage sources $U_C(i, j)$ and a pairs of 3 turn-on and turn-off controlled semiconductor devices $T(i, j)$ and $T'(i, j)$ which have complementary states. Each flying capacitor $C(i, j)$ is connected between the pairs of switches $T(i, j+1)$, $T(i, j)$ controlled by the control signal $S(i, j + 1)$ and $S(i, j)$ [19, 20].
$i \in [1, 2, 3]$ and $j \in [1, p]$ (for N levels inverter the number of the commutations cells is given by $p = N - 1$).

The per phase output voltage of the four level inverter U_{AN}, U_{BN} and U_{CN}, are expressed in terms of the flying capacities voltages $[\Delta Uc]_i$ and the switching function S_{phi} [19] as:

$$\begin{bmatrix} U_{AN} \\ U_{BN} \\ U_{CN} \end{bmatrix} = \frac{1}{3}\begin{bmatrix} 2 & -1 & -1 \\ -1 & 2 & -1 \\ -1 & -1 & 2 \end{bmatrix}\begin{bmatrix} [\Delta Uc]_1 & [000] & [000] \\ [000] & [\Delta Uc]_2 & [000] \\ [000] & [000] & [\Delta Uc]_3 \end{bmatrix}\begin{bmatrix} [S_{ph1}] \\ [S_{ph2}] \\ [S_{ph3}] \end{bmatrix} \quad (1)$$

The Clark transformation $[T_{32}]$ is used to pass from the three-phase voltages system $[U_{AN}U_{BN}U_{CN}]^T$ to an equivalent two-phase system [19], such as

$$\begin{bmatrix} U_{S\alpha} \\ \\ U_{S\beta} \end{bmatrix} = [B_1].[U]; \quad dim[B_1] = (2, 9) \quad (2)$$

With:

$$[U] = \begin{bmatrix} [S_{ph1}] \\ [S_{ph2}] \\ [S_{ph3}] \end{bmatrix}; Dim\,[U] = 9 \quad (3)$$

$$[B_1] = \frac{2}{3}\begin{bmatrix} [\Delta U_C]_1 & -\frac{1}{2}[\Delta U_C]_2 & -\frac{1}{2}[\Delta U_C]_3 \\ \\ [000] & \frac{\sqrt{3}}{2}[\Delta U_C]_2 & -\frac{\sqrt{3}}{2}[\Delta U_C]_3 \end{bmatrix} \quad (4)$$

4. Flying Capacities Voltages Evolutions

In order to describe the influence of the different states of the switches $T(i, j)$, $T'(i, j)$, $T(i, j + 1)$ and $T'(i, j + 1)$ on the evolution of the flying capacities voltages $U_C(i, j)$ and on the currents $Ic(i, j)$ as shown in figure 2, we analyse the current in each capacity $C(i, j)$ for various possible states of the switches. This analytic study is developed in [18, 19, 20] and gives in equations (5) and (6) the relations between $C(i, j)$, $Ic(i, j)$, $Uc(i, j)$ and $S(i, j)$

$$\frac{d}{dt}\begin{bmatrix} Uc(1,1) \\ Uc(1,2) \\ Uc(2,1) \\ Uc(2,2) \\ Uc(3,1) \\ Uc(3,2) \end{bmatrix} = [B_2].[U]; dim[B_2] = (6, 9) \quad (5)$$

With:

$$[B_2] = \begin{bmatrix} -\frac{I_1}{C(1,1)} & \frac{I_1}{C(1,1)} & 0 & 0 & 0 & 0 & 0 & 0 & 0 \\ 0 & -\frac{I_1}{C(1,2)} & \frac{I_1}{C(1,2)} & 0 & 0 & 0 & 0 & 0 & 0 \\ 0 & 0 & 0 & -\frac{I_2}{C(2,1)} & \frac{I_2}{C(2,1)} & 0 & 0 & 0 & 0 \\ 0 & 0 & 0 & 0 & -\frac{I_2}{C(2,2)} & \frac{I_2}{C(2,2)} & 0 & 0 & 0 \\ 0 & 0 & 0 & 0 & 0 & 0 & -\frac{I_3}{C(3,1)} & \frac{I_3}{C(3,1)} & 0 \\ 0 & 0 & 0 & 0 & 0 & 0 & 0 & -\frac{I_3}{C(3,2)} & \frac{I_3}{C(3,2)} \end{bmatrix} \quad (6)$$

$[B_2]$ is a nonlinear matrix. This nonlinearity as shown in equation (6) is caused by the dependence between flying capacities voltages and stator currents I_1, I_2 and I_3 evolutions [18, 19].

5. System Modelling by Taking into Account Flying Capacities Voltages Variations

The state-space representation of the induction motor-four level inverter system in (α, β) stationary reference frame is given by:

$$\frac{dX}{dt} = [A\,(X)]X + [B(X)]\,U \quad (7)$$

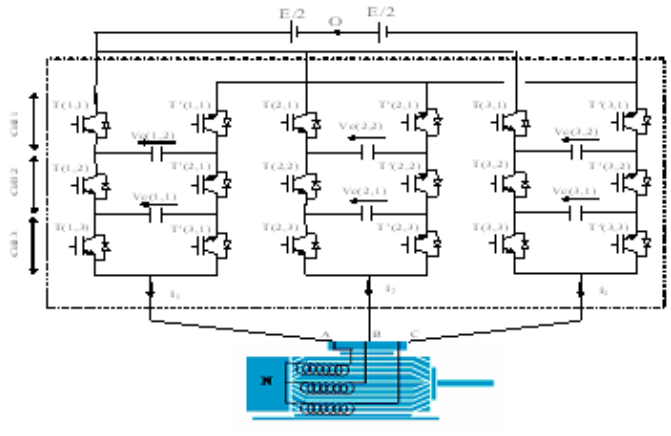

Fig. 1. Four level inverter fed induction motor.

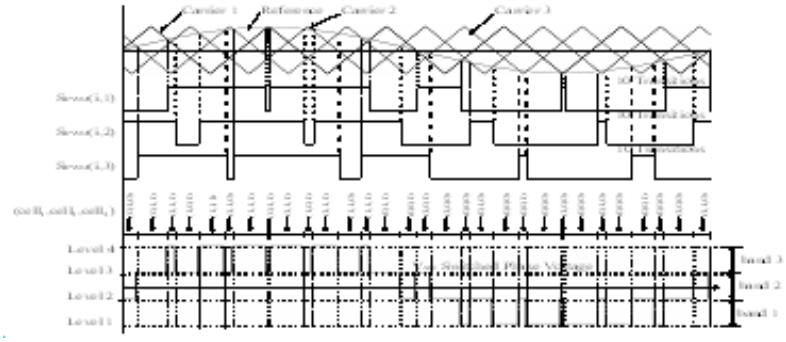

Fig. 2. Phase Shifted Carrier PWM for a four level inverter.

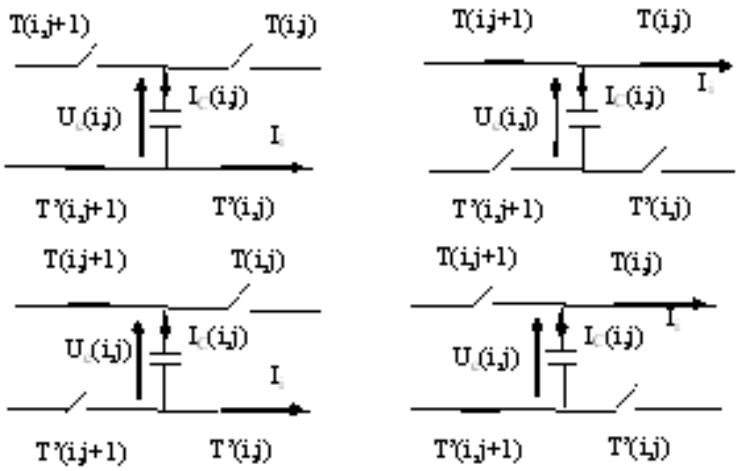

Fig. 3. All possible states of switches on both sides of the capacitor $C(i, j)$.

The state space vector X is composed by six flying capacities voltages, two stators current components, two rotors flux components, and the angular speed ω, such as:

$$X = [\ [U_C^{(i,j)}\ ]^T\ [i_S]^T\ [\varphi_r]^T \omega\ \ ]^T \tag{8}$$

With:

$$dim[U_C(i,j)]^T = (3p-3,1) = (6,1)$$

$$[i_S] = [i_{s\alpha}\ i_{s\beta}]^T$$

$$[\Phi_r] = [\varphi_{r\alpha}\ \varphi_{r\beta}]^T$$

The control vector U is composed by the commutations cells control signals $S(i, j)$, given by:

$$U = [S(1,j), S(2,j), S(3,j)]^T \quad \text{With} \quad dim[U] = (9,1)$$

Equation (9) represents the state matrix such as:

$$[A]=\begin{bmatrix} 0 & \cdots & \cdots & 0 \\ \vdots & \cdots & \cdots & \vdots \\ 0 & \cdots & 0 & 0 \\ 0 & \cdots & 0 & [A_M] \end{bmatrix} \tag{9}$$

With:

$$dim[A] = (11, 11) \quad \text{And} \quad dim[A_M] = (5, 5)$$

And:

$$[A_M]=\begin{bmatrix} -\gamma & 0 & \frac{K}{T_r} & 0 & p_n K\varphi_{r\beta} \\ 0 & -\gamma & 0 & \frac{K}{T_r} & -p_n K\varphi_{r\alpha} \\ \frac{M}{T_r} & 0 & -\frac{1}{T_r} & 0 & -p_n\varphi_{r\beta} \\ 0 & \frac{M}{T_r} & 0 & -\frac{1}{T_r} & p_n\varphi_{r\alpha} \\ 0 & 0 & \mu i_{S\beta} & -\mu i_{S\alpha} & -\frac{f}{J} \end{bmatrix} \tag{10}$$

The system modelling in terms of the flying capacities voltages variations is given by:

$$\begin{bmatrix} \dot{U}_c(1,1) \\ \dot{U}_c(1,2) \\ \dot{U}_c(2,1) \\ \dot{U}_c(2,2) \\ \dot{U}_c(3,1) \\ \dot{U}_c(3,2) \\ \dot{i}_{s\alpha} \\ \dot{i}_{s\beta} \\ \dot{\varphi}_{r\alpha} \\ \dot{\varphi}_{r\beta} \\ \dot{\omega} \end{bmatrix} = [A] \begin{bmatrix} U_c(1,1) \\ U_c(1,2) \\ U_c(2,1) \\ U_c(2,2) \\ U_c(3,1) \\ U_c(3,2) \\ i_{s\alpha} \\ i_{s\beta} \\ \varphi_{r\alpha} \\ \varphi_{r\beta} \\ \omega \end{bmatrix} + [B(X)] \begin{bmatrix} S(1,1) \\ S(1,2) \\ S(1,3) \\ S(2,1) \\ S(2,2) \\ S(2,3) \\ S(3,1) \\ S(3,2) \\ S(3,3) \end{bmatrix} \tag{11}$$

The control matrix $B(x)$ is deduced from equations (4) and (6) and given by:

$$[B(X)]=\begin{bmatrix} [B_2(X)] \\ \frac{[B_1(X)]}{\sigma L_s} \\ 000000000 \\ 000000000 \\ 000000000 \end{bmatrix} \tag{12}$$

With:

$$Dim([B(x)]) = (11, 9).$$

Based on system modelling, we can see clearly the nonlinearity in the state and in the control matrices [19, 20]. The first is caused by the strong coupling between induction motor variables states and the second is due to the power devices components nonlinearity. Input output linearization technique-based system control has presented a singularity in calculation. To overcome this one, an algorithm is developed and presented in Section 6.

6. Control Algorithm Development

The proposed algorithm shown by figure 4 is constituted by two blocks diagrams. The first one aims to resolve the state matrix nonlinearity. A nonlinear decoupling control based on feedback linearization theory is developed to control and decouple rotor flux and angular speed. Input-output feed back control presented into block1 will generate thereafter the three references voltages U_{1ref}, U_{2ref} and U_{3ref}. Flying capacities voltages stabilization based on PI regulators is presented into the second block diagram. As a result, these two blocks diagrams are combined to generate the PWM four level inverter controls to feed induction motor [19].

The decoupling control system based on Input-output linearization consists to develop a static feed back [21, 22] described by equation (13) and schematized by figure 5 presented below:

$$u = \alpha(x) + \beta(x)\, v \tag{13}$$

Based on algorithm control, the induction motor variables states to be controlled are the rotor flux modulus square given by $\Phi=\varphi_{r\alpha}^2+\varphi_{r\beta}^2$ and the angular speed ω.

For the control design, the complete state space model is given in the form of equation (A.35) and equation (A.36) as follows.

$$y=\begin{bmatrix} y_1 \\ y_2 \end{bmatrix}=\begin{bmatrix} h_1(x) \\ h_2(x) \end{bmatrix}=\begin{bmatrix} \omega \\ \Phi \end{bmatrix}=\begin{bmatrix} \omega \\ \varphi_{r\alpha}^2+\varphi_{r\beta}^2 \end{bmatrix} \tag{14}$$

Proceeding with the exact steps as outlined in the Appendix A, the followings can be derived.

$$\dot{h}_1(x) = L_f h_1(x) = \dot{\omega} \tag{15}$$

$$\ddot{h}_1(x) = L_f^2 h_1(x) + L_{g1} L_f h_1(x)\ U_{s\alpha} + L_{g2} L_f h_1(x)\ U_{s\beta} \tag{16}$$

And:

$$\dot{h}_2(x) = L_f h_2(x) = \Phi \tag{17}$$

$$\ddot{h}_2(x) = L_f^2 h_2(x) + L_{g1} L_f h_2(x)\ U_{s\alpha} + L_{g2} L_f h_2(x)\ U_{s\beta} \tag{18}$$

With:

$$L_f^2 h_1(x) = \mu(\gamma + \frac{f}{J} + \frac{1}{T_r})(i_{s\alpha}\varphi_{r\beta} - i_{s\beta}\varphi_{r\alpha}) - p_n k\,\mu(\varphi_{r\alpha}^2 + \varphi_{r\beta}^2)\omega - p_n\mu(i_{s\alpha}\varphi_{r\beta} + i_{s\beta}\varphi_{r\alpha})\omega + (\frac{f}{J})^2\omega + \frac{f\,T_L}{J^2} \tag{19}$$

And:

$$L_{g1} L_f h_1(x) = \frac{-p_n K}{J}\varphi_{r\beta} \tag{20}$$

$$L_{g2} L_f h_1(x) = \frac{p_n K}{J}\varphi_{r\alpha} \tag{21}$$

$$L_f^2 h_2(x) = 2\left[\left(\frac{M}{T_r}\right)^2\left(i_{s\alpha}^2 + i_{s\beta}^2\right) - \left(\frac{3M}{T_r^2} + \frac{\gamma M}{T_r}\right)(i_{s\alpha}\varphi_{r\alpha} + i_{s\beta}\varphi_{r\beta}\right) + \left(\frac{2}{(T_r)^2} + \frac{Mk}{(T_r)^2}\right)\left(\varphi_{r\alpha}^2 + \varphi_{r\beta}^2\right) - \frac{M p_n}{T_r}\left(i_{s\alpha}\varphi_{r\beta} - i_{s\beta}\varphi_{r\alpha}\right)\omega\Big] \tag{22}$$

$$L_{g1} L_f h_2(x) = 2R_r K\varphi_{r\alpha} \tag{23}$$

$$L_{g2} L_f h_2(x) = 2R_r K\varphi_{r\beta}. \tag{24}$$

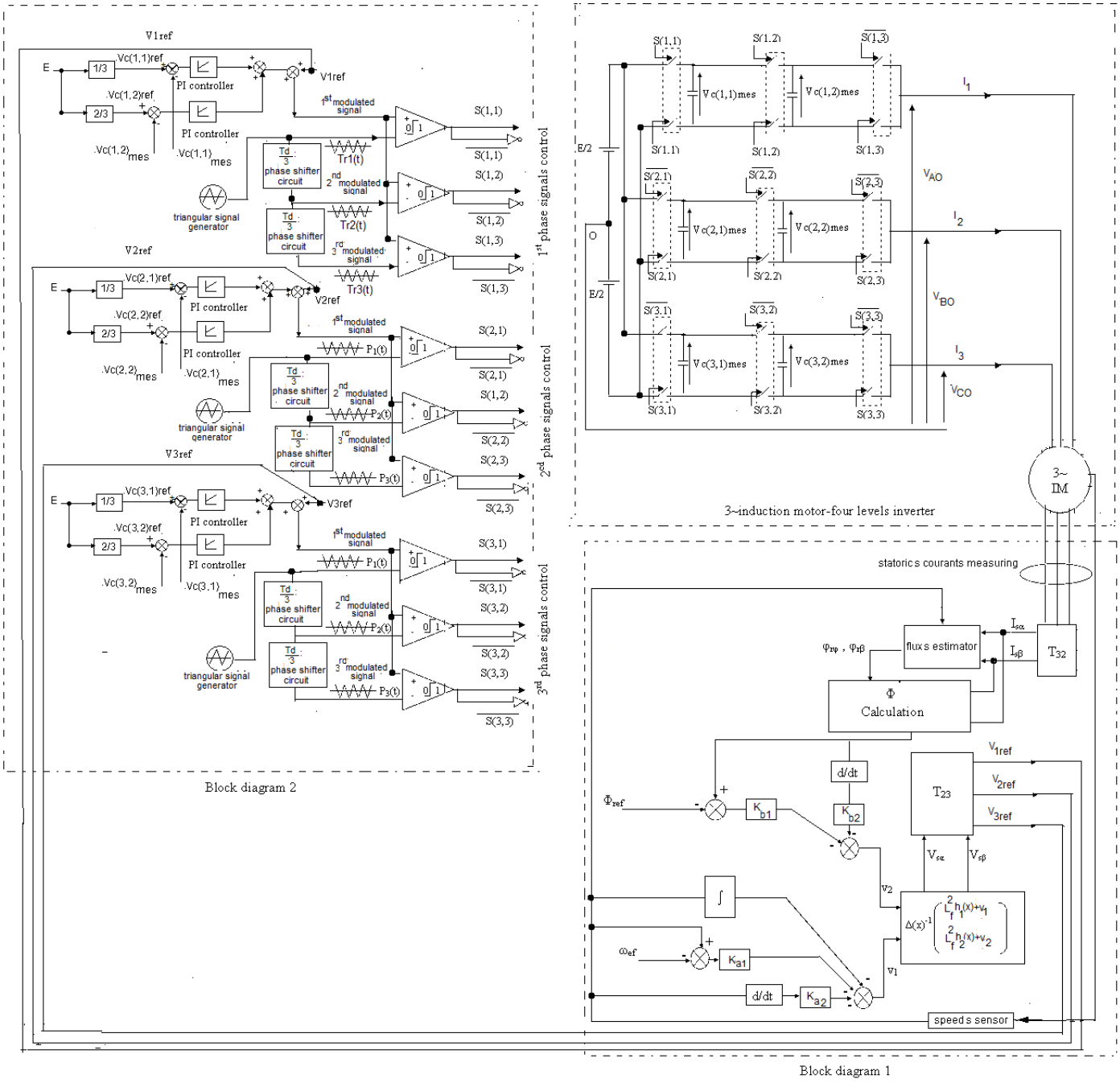

Fig. 4. Control algorithm scheme of the induction motor-four level inverter system; block diagram 1: rotor flux and angular decoupling control; Block diagram 2: PI controllers in opened loop to stabilize the four level inverter flying capacities voltages.

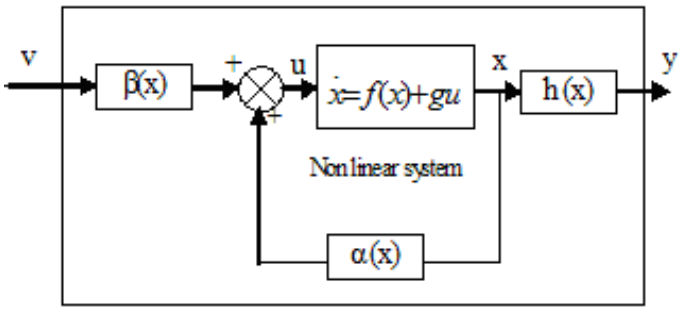

Fig. 5. Input-output linearization system diagram.

Feed back regulation dynamic of the decoupled and linearized system is given in step with the newly control vectors v1 and v2 as:

$$\begin{cases} \ddot{h}_1(x) = v_1 \\ \ddot{h}_2(x) = v_2 \end{cases} \tag{25}$$

The system can be rewritten as the following form:

$$\begin{bmatrix} \ddot{h}_1(x) \\ \ddot{h}_2(x) \end{bmatrix} = \begin{bmatrix} L_f^2 h_1(x) \\ L_f^2 h_2(x) \end{bmatrix} + \Delta(x) \begin{bmatrix} U_{S\alpha} \\ U_{S\beta} \end{bmatrix} \tag{26}$$

The control decoupling matrix $\Delta(x)$ is given by:

$$\Delta(x) = \begin{bmatrix} \frac{-p_n K \varphi_{r\beta}}{J} & \frac{p_n K \varphi_{r\alpha}}{J} \\ 2R_r K \varphi_{r\alpha} & 2R_r K \varphi_{r\beta} \end{bmatrix} \tag{27}$$

$$\Delta^{-1}(x) = \begin{bmatrix} -\frac{J\varphi_{r\beta}}{Kp_n(\varphi_{r\alpha}^2+\varphi_{r\beta}^2)} & \frac{\varphi_{r\alpha}}{2K.R_r(\varphi_{r\alpha}^2+\varphi_{r\beta}^2)} \\ \frac{J\varphi_{r\alpha}}{K.p_n(\varphi_{r\alpha}^2+\varphi_{r\beta}^2)} & \frac{\varphi_{r\beta}}{2K.R_r(\varphi_{r\alpha}^2+\varphi_{r\beta}^2)} \end{bmatrix} \tag{28}$$

The decoupling matrix is singular only if $\Phi = 0$ [19, 23].This singularity is taking place only at the motor start up. It proves to be necessary to provide an open loop control law such as the conventional constant volts per hertz law, known as U/f control, during the motor start up phase and to lock up the system on the feed back linearization control when there's an appearance of a minimal flux Φ [24, 25]. If the decoupling matrix is non singular, the feed back non-linear control is given by:

$$\begin{aligned} \begin{bmatrix} U_{S\alpha} \\ U_{S\beta} \end{bmatrix} &= \Delta(x)^{-1} \begin{bmatrix} -L_f^2 h_1(x) + v_1 \\ -L_f^2 h_2(x) + v_2 \end{bmatrix} \\ &= \Delta(x)^{-1} \begin{bmatrix} -L_f^2 h_1(x) \\ -L_f^2 h_2(x) \end{bmatrix} + \Delta^{-1}(x) \begin{bmatrix} v_1 \\ v_2 \end{bmatrix} \\ &= \alpha(x) + \beta(x) \begin{bmatrix} v_1 \\ v_2 \end{bmatrix} \end{aligned} \tag{29}$$

Such as:

$$\begin{cases} \alpha(x) = \Delta(x)^{-1} \begin{bmatrix} -L_f^2 h_1(x) \\ -L_f^2 h_2(x) \end{bmatrix} \\ \beta(x) = \Delta(x)^{-1} \end{cases} \tag{30}$$

And:

$$\begin{bmatrix} -L_f^2 h_1(x) + v_1 \\ -L_f^2 h_2(x) + v_2 \end{bmatrix} = \begin{bmatrix} -\mu(\gamma + \frac{f}{J} + \frac{1}{T_r})(i_{s\alpha}\varphi_{r\beta} - i_{s\beta}\varphi_{r\alpha}) + p_n K \mu \Phi \omega \\ +p_n \mu (i_{s\alpha}\varphi_{r\alpha} + i_{s\beta}\varphi_{r\beta})\omega - \frac{f^2}{J^2}\omega - \frac{fT_L}{J^2} + v_1 \\ -\frac{2M^2(i_{s\alpha}^2+i_{s\beta}^2)}{T_r} + 2(\frac{3M}{T_r^2} + \frac{\gamma M}{T_r})(i_{s\alpha}\varphi_{r\beta} - i_{s\beta}\varphi_{r\alpha}) \\ -2(\frac{2}{T_r^2} + \frac{Mk}{T_r^2})\Phi + \frac{2Mp_n(i_{s\alpha}\varphi_{r\alpha}+i_{s\beta}\varphi_{r\beta})\omega}{T_r} + v_2 \end{bmatrix} \tag{31}$$

Figure 6 represents the structure of the proposed non-linear regulator.

For tracking $U_{s\alpha}$ and $U_{s\beta}$, the newly inputs control vectors v1 and v2 are selected by proportional and integral regulators control [4, 19], such as:

$$\begin{cases} v_1 = -k_{a1}(\omega - \omega_{ref}) - k_{a2}\dot{\omega} - \int_0^t \omega dt \\ v_2 = -k_{b1}(\Phi - \Phi_{ref}) - k_{b2}^{\dot{\Phi}} \end{cases} \tag{32}$$

The constant parameters K_{a1}, K_{a2}, K_{b1} and K_{b2} are calculated and selected such as the system in a feed back control is stable and satisfy high dynamic performances [25].

As result, the expressions of the control vectors are given by:

$$\begin{aligned} U_{s\alpha} = {} & \frac{-\varphi_{r\beta} J}{K p_n \Phi}\Big[-\mu(\gamma + \frac{f}{J} + \frac{1}{T_r})(i_{s\alpha}\varphi_{r\beta} - i_{s\beta}\varphi_{r\alpha} + p_n K \mu) \\ & \times (\Phi\omega + p_n \mu (i_{s\alpha}\varphi_{r\beta} + i_{s\beta}\varphi_{r\alpha})\omega) - \frac{f^2}{J^2}\omega - \frac{fT_L}{J^2} + v_1\Big] \\ & + \frac{\varphi_{r\alpha}}{2KR_r\Phi}\Big[-\frac{2M^2(i_{s\alpha}^2 + i_{s\beta}^2)}{T_r^2} + 2(\frac{3M}{T_r^2 + \frac{\gamma M}{T_r}}) \\ & (i_{s\alpha}\varphi_{r\beta} + i_{s\beta}\varphi_{r\alpha}) - 2(\frac{2}{T_r^2} + \frac{Mk}{T_r^2})\Phi \\ & + \frac{2Mp_n((i_{s\alpha}\varphi_{r\beta} - i_{s\beta}\varphi_{r\alpha})\omega}{T_r} + v_2\Big] \end{aligned} \tag{33}$$

$$\begin{aligned} U_{S\beta} = {} & \frac{\varphi_{r\alpha} J}{K p_n \Phi}\Big[-\mu(\gamma + \frac{f}{J} + \frac{1}{T_r})(i_{s\alpha}\varphi_{r\beta} - i_{s\beta}\varphi_{r\alpha}) \\ & + p_n K \mu \Phi \omega + p_n \mu (i_{s\alpha}\varphi_{r\beta} + i_{s\beta}\varphi_{r\alpha})\omega - \frac{f^2}{J^2}\omega - \frac{fT_L}{J^2} + v_1\Big] \\ & + \frac{\varphi_{r\beta}}{2KR_r\Phi}\Big[-\frac{2M^2(i_{s\alpha}^2 + i_{s\beta}^2)}{T_r^2} + 2(\frac{3M}{T_r^2} + \frac{\gamma M}{T_r}) \\ & (i_{s\alpha}\varphi_{r\beta} + i_{s\beta}\varphi_{r\alpha}) - 2(\frac{2}{T_r^2} + \frac{Mk}{T_r^2})\Phi \\ & + \frac{2Mp_n((i_{s\alpha}\varphi_{r\beta} - i_{s\beta}\varphi_{r\alpha})\omega)}{T_r} + v_2\Big] \end{aligned} \tag{34}$$

7. Simulation Results and Discussion

Simulation parameters are: DC link bus voltage E = 600 V, flying capacitors voltages values $Uc(i,j)_{ref}$ = jE/3 with j∈[1, 2, 3], output frequency = 50 Hz,Triangular Carrier period and frequency T_d = 400 us and f_d = 2.5 k Hz, induction motor nominal power P_n = 45 Kw, nominal angular speed ω_n = 153 rad/s, pairs of poles pn=2. To obtain a fast and stable answer on speed and flux, the PI regulators parameters are selected such as: K_{a1}= 3, K_{a2}= 610^3, K_{b1} = 1.7510^6 and K_{b2} = 70.

Algorithm-based simulation results, present in Fig.8, Fig.9 and in Fig 10 angular speed, modulus square rotor flux and stator current respectively, at nominal and decelerated functioning mode before and after load torque application (decelerated mode corresponds to $\omega_n/5$).

Fig. 11 and Fig. 12 given below represents angular speed and rotor flux behaviors at nominal and accelerated functioning mode, before and after load torque (accelerated mode corresponds to $4\omega_n/3$).

During the accelerated functioning mode we defluxed the motor in order to keep its functioning in a constant power witch corresponds to the nominal one.

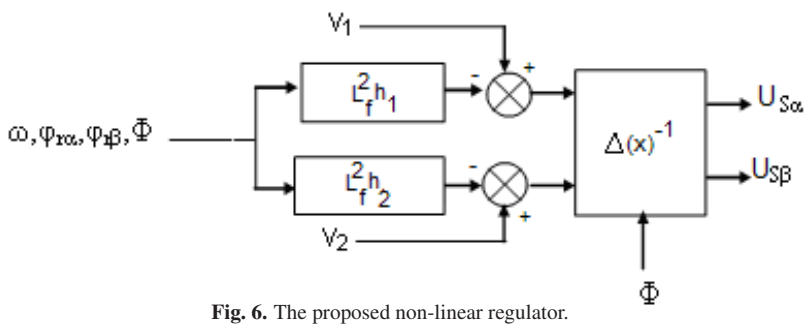

Fig. 6. The proposed non-linear regulator.

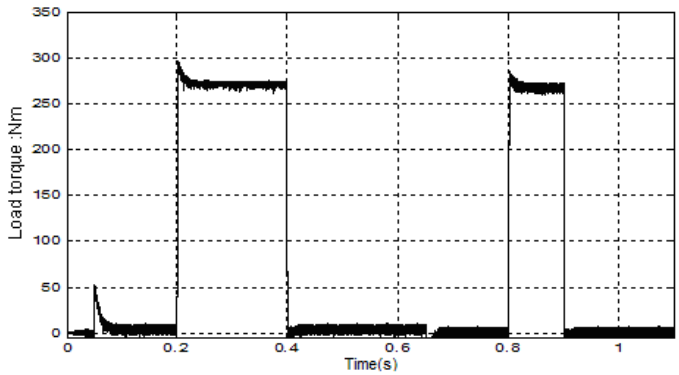

Fig. 7. Induction motor electromagnetic torque before and after load torque: Time interval of load torque application [0.2s .04s] and [0.8s 0.9s].

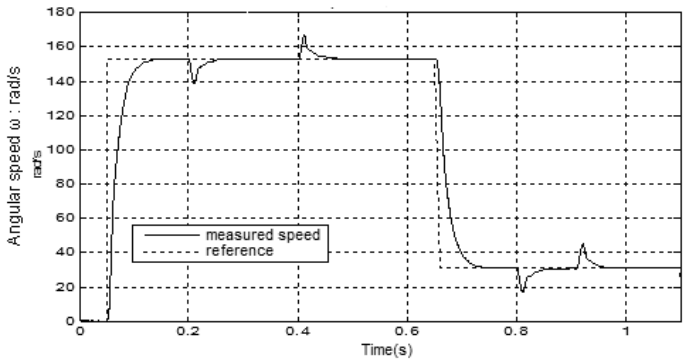

Fig. 8. The behavior of the angular speed before and after load torque for nominal and decelerated functioning: nominal and decelerated speed intervals times [0.05s 0.65s] and [0.65s 1.1s]s respectively.

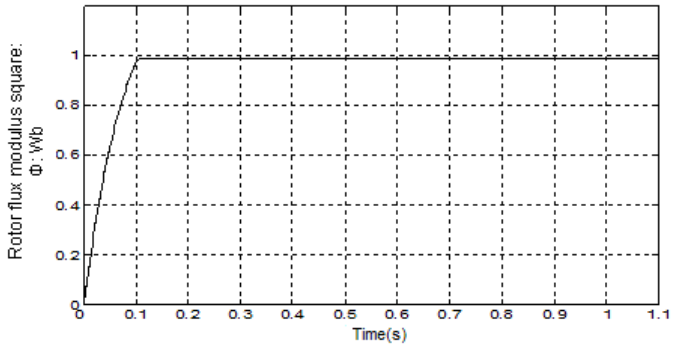

Fig. 9. Rotor flux square modulus behavior in nominal and decelerated mode after and before load torque.

Fig. 13 represents the per phase four level flying capacities voltages Uc(1,1) and Uc(1,2) for references values: Uc(1,1) ref = 200 and Uc(1,2) = 400 V.

Fig. 14 represents the phase to phase four level inverter output voltages.

Based on the obtained simulation results, we can deduce:

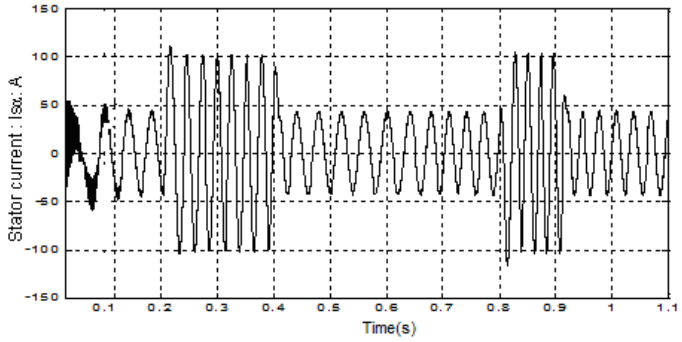

Fig. 10. Stator current evolution after and before load torque.

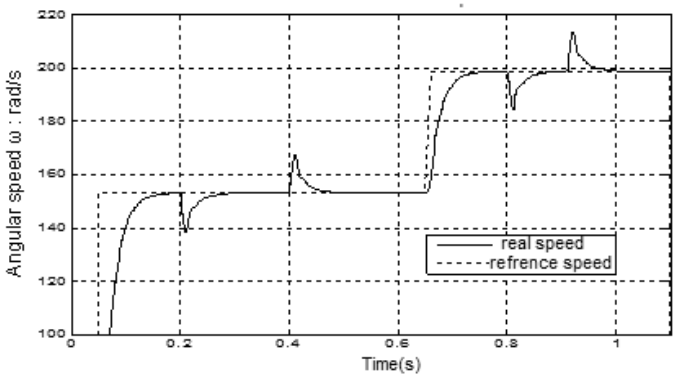

Fig. 11. Angular speed before and after load torque for nominal and accelerated mode: nominal and accelerated speed intervals times [0.05 s 0.65 s] and [0.65s 1.1s] respectively.

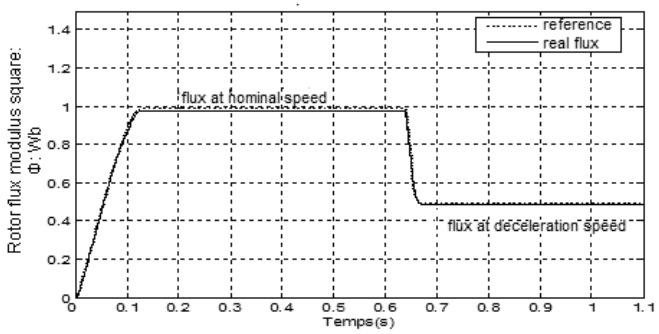

Fig. 12. Rotor flux square modulus at nominal and defluxed mode at nominal and decelerated speed functioning during intervals times [0.1s 0.65s] and [0.65s 1.1s] respectively.

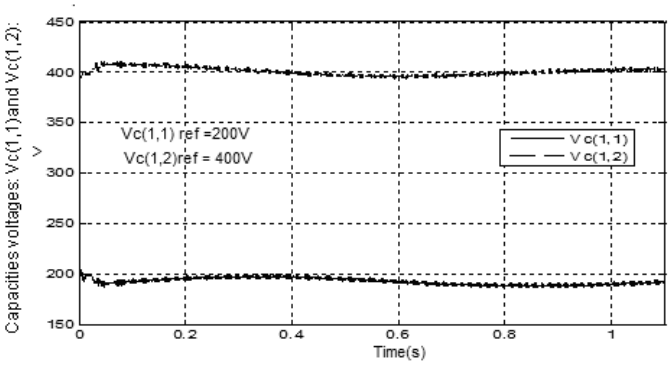

Fig. 13. The 1st phase flying capacities voltages Vc(1,1) and Vc(1,2).

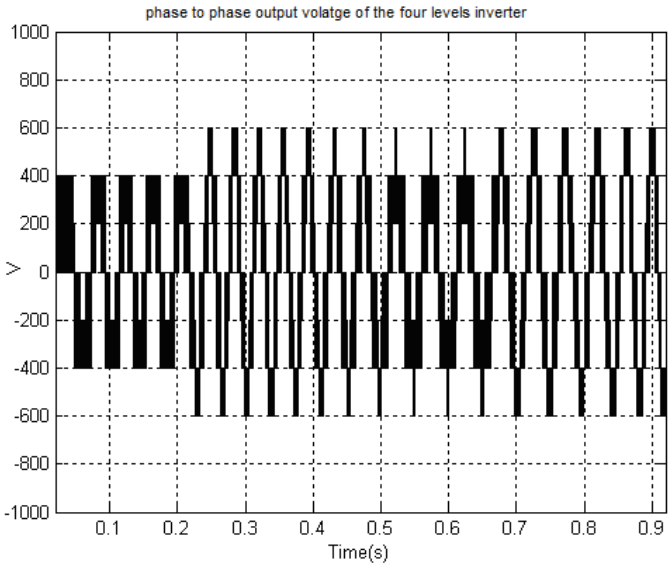

Fig. 14. Phase to phase output voltage of the 4 levels inverter.

- The load torque acting on the induction motor speed is quickly compensated by the proposed regulators with a stabilisation time lower than 1s in nominal, accelerated and decelerated functioning mode.
- Speed and flux reaches their desired references values with a speed fall lower than 2%.
- A perfect decoupling between speed and flux even in the rotor flux transient.
- The insertion of the load torque affects speed without however affecting flux.
- A reasonable evolution of the stator current before and after load torque

Fig. 11 shows that the speed is insensitive to the rotor flux variations even in a defluxed mode. This confirms the control algorithm efficacy to allow a full decoupling of rotor flux and speed control. Speed error does not exceed 1 % and it remains lower than that desired in several applications with a high performances.

In Fig 13, the flying capacities voltages are balanced, stables and reached their references with an undulation lower than 5%

In fig 14 the phase to phase output voltage of the four level inverter presents four level voltages: 0, E/3, 2E/3 and E

8. Conclusion

A new approach is developed to control multilevel inverter-induction motor system based on input-output linearization theory. Speed and flux decoupling control by assuring flying capacities voltages stabilization are our objectives in this paper. Algorithm control law has been tested through simulation in accelerated, decelerated speed and in defluxed mode. Simulation results show that the proposed algorithm allows speed and flux decoupling control and flying capacities voltages regulation simultaneously with high performances dynamic. The results obtained show that this technique may overcome some difficulties related to multilevel inverter-induction motor system control.

9. List of symbols

M: mutual inductance

Rs, Rr: the stator and rotor resistance respectively

Ls, Lr: the stator and rotor self-inductance respectively

Ts=Ls/Rs, Tr=Lr/Rr: Stator and Rotor time constant

σ =(1-M^2/Ls/Lr): Leakage factor

K=M/(σLsLr)

γ =Rs/(σLs)+RsM^{2}sr/(σLsLr); μ=3p^2/(2JLr)

ω : induction motor angular speed

$\phi_{r\alpha}$ and $\phi_{r\beta}$: 2 phase rotor flux linkages

$i_{s\alpha}$ and $i_{s\beta}$: 2 phase stator current

f : Viscous friction coefficient

pn: number of pole pairs

J: inertia moment coefficient

T_L: load torque

i $\in$ [1, 2, 3] for the three phases

j $\in$ [1 . . . p] for the number of cells in each phase

$T(i, j)$ & $T'(i, j)$: Two Power semiconductor switches for the ith phase jthcell having complementary switching signal

$S(i, j)$: switching signal of $T(i, j)$

$S'(i, j)$: switching signal of $T'(i, j)$, complementary of $S(i, j)$

$C(i, j)$: flying capacitor for the ith phase j^{th} cell

$U_T(i, j)$: voltage across the switch $T(i, j)$

Uc(i,j): voltage across flying capacitor for the ith phase jth cell

E: DC bus voltage in the input of the inverter

U_{AO}, U_{BO}, U_{CO}: the voltages between each phase and the middle point of the DC input source

U_{AB},U_{BC},U_{CA}: voltages between two consecutives phases

References

[1] S.-S. Ge, Z. Sun, and T.-H. Lee, "Nonregular feedback linearization for a class of second-order nonlinear systems," *Automatica*, vol. 37, pp. 1819–1824, 2001.

[2] H. Sira-Ramirez and M. Ilic-Spong, "Exact linearization in switched mode DC to DC power converters," *Electrical Power and Energy Systems*, vol. 26, pp. 37–48, 2004.

[3] M. K. Maaziz, E. Mendesb, and P. Boucher, "A new nonlinear multivariable control strategy of induction motors.," *Control Engineering Practice*, vol. 10, pp. 605–613, 2002.

[4] D.-I. Kim, I.-J. Ha, and M.-S. Ko, "Control of induction motor via feedback linearization with input-output decoupling.," *International Journal of Control*, vol. 51, pp. 863–86, 1990.

[5] J.-W. Chapman, M.-D. Ilic, C. King, L. Eng, and H. Haufman, "Stabilizing a multi-machine power system via decentralized feedback linearizing excitation control," *IEEE Transactions on System Power System*, vol. 8, pp. 830–839, 1993.

[6] B.-R. Lin, "High power factor ac/dc/ac converter with h-bridge cascade five-level PWM inverter," *European Transactions on Electrical Power*, vol. 11, pp. 97–106, 2001.

[7] B. P. McGrath and D. G. Holmes, "Analytical modelling of voltage balance dynamics for a flying capacitor multilevel converter," *IEEE Transactions on Power Electron*, vol. 23, no. 2, pp. 543–550, 2008.

[8] A. Meynard, H. Foch, F. Forest, C. Turpin, F. Richardeau, L. Delmas, G. Gateau, and E. Lefeuvre, "Multicell converters: derived topologies," *IEEE Transactions on Industrial Electronics*, vol. 49, no. 5, pp. 978–987, 2002.

[9] A. Meynard, H. Foch, P. Thomas, J. Courault, R. Jackob, and M. Nahrstaed, "Multicell converters: basic concepts and industry applications," *IEEE Transactions on Industrial Electronics*, vol. 49, no. 5, pp. 955–1964, 2002.

[10] G. Gateau, M. Fadel, P. Maussion, R. B. Said, and T. A. Meynard, "Multicell converters: active control and observation of flying capacitor voltages," *IEEE Transactions on Industrial Electronics*, vol. 49, no. 5, pp. 998–1007, 2002.

[11] J. Rodriguez, J.-S. Lai, and F. Z. Peng, "Multilevel inverters: a survey of topologies, controls, and applications," *IEEE Transactions on Industrial Electronics*, vol. 49, pp. 724–738, 2002.

[12] S. Khomfoi and L. M. Tolbert, "Fault diagnosis and reconfiguration for multilevel inverter drive using AI-based techniques," *IEEE Transactions on Industrial Electronics*, vol. 54, no. 6, pp. 2954–2968, 2007.

[13] L. M. Tolbert and T. G. Habetler, "Novel multilevel inverter carrier-based PWM method," *IEEE Transactions on Industry Applications*, vol. 35, pp. 1098–1107, 1999.

[14] G. Chao, "A class of high-performance multi-level power factor correct switching converter based on predictive control technology:analysis, design and experiment," *International Conference On Advanced Information Technology*, 2008.

[15] S. T. S and Y. Tatar, "A new approach for selecting the switching states of SVPWM algorithm in multilevel inverter," *European Transactions on Electrical Power*, vol. 17, pp. 81–95, 2007.

[16] H. Chekireb and E.-M. Berkouk, "Generalised algorithm of novel space vector modulation: for N-level three-phase voltage source inverter," *European Transactions on Electrical Power*, vol. 18, pp. 127–150, 2008.

[17] M. S. A. Dahidah, V. G. Agelidis, and G. Agelidis, "Single-carrier sinusoidal PWM-equivalent selective harmonic elimination for a five-level voltage source converter," *Electric Power Systems Research*, vol. 78, pp. 1826–1836, 2008.

[18] F. B. Ammar, M. B. Smida, and L. Manai, "Filtrage actif shunt des réseaux électriques moyenne tension avec des convertisseurs de puissance multiniveaux," *Revue Inernationale en Ggnie Electrique*, vol. 8, pp. 377– 406, 2005.

[19] L. Manai, *Alimentation d'une machine à induction de grande puissance par des convertisseurs multiniveaux*. PhD thesis, National Engineering School of tunis (ENIT)-Tunisia, 2008.

[20] L. Manai and F. B. Ammar, "Approche d'une commande par retour d'état par la méthode de la linéarisation entrée-sortie de l'association convertisseur multiniveaux-machine asynchrone triphasée," in *CRATT 2007 1ère conférence internationale* (Tunisia, ed.), Rades, 14&15 November 1999.

[21] A. D. Luca and G. Ulivi, "Design of exact nonlinear controller for induction motors," *IEEE Transactions on Automatic Control*, vol. 34, pp. 1304–1307, 2007.

[22] T. V. Raumer, J. M. Dion, L. Dugard, and J. L. Thomas, "Applied nonlinear control of an induction motor using digital signal processing," *IEEE Transactions on Control System*, vol. 2, pp. 327–335, 1994.

[23] V. G. D. C. Samarasinghe and N. C. Pahalawaththa, "Stabilization of a multi-machine power system using nonlinear robust variable structure control," *Electric Power Systems Research*, vol. 43, no. 1, pp. 11–17, 1997.

[24] Y. L. Tan and Y. Wang, "Design of series and shunt FACTS controller using adaptive nonlinear coordinated design techniques," *IEEE Transactions on Power System*, vol. 12, no. 1, pp. 374–1379.

[25] D. Chunyan, X. Xu, S. P. Banks, and A. Wu, "Control of nonlinear functional differential equations," *Nonlinear Analysis: Theory, Methods & Applications*, vol. 71, no. 12, pp. 1850–1857, 2009.

Appendix A

Feedback linearization control

A brief review of nonlinear control using feedback linearization without loss of generality, the following MIMO (multiple input and multiple output) system is considered is presented here.

Consider a multivariable nonlinear system:

$$\dot{x} = f(x) + \sum_{i=1}^{m} g_i(x) u_i \tag{A.35}$$

$$y = h(x) \tag{A.36}$$

where $x(\in R^n)$ is state vector, $u(\in R^m)$ represents control inputs, $y(\in R^m)$ stands for outputs, f and g are smooth vector fields, and h is a smooth scalar function. The input–output linearization of the above MIMO system is achieved by differentiating y of the system until the inputs appear explicitly. Thus, by differentiating (A2),

$$\dot{y}_i = L_f h_i + \sum_{j=1}^{m} (l_{gj} h_i) u_j \; ; i = 1, \ldots, m \tag{A.37}$$

Where $L_f h$ and $L_g h$ represent the Lie derivatives of $h(x)$ with respect to $f(x)$ and $g(x)$, respectively. The key point is that, if $L_{gj} L_f^{(r_i-1)} h_i(x) = 0$ for all j, then the inputs do not appear in (A.37) and further differentiation is to be repeated as:

$$y_i^{r_i} = L_f^{(r_i)} h_i + \sum_{j=1}^{m} (L_{g\,j} L_f^{(r_i-1)} h_i) u_j ; i = 1, \ldots, m \tag{A.38}$$

Such that $L_{gj} L_f^{(r_i-1)} h_i(x) = 0$ for at least one j. This procedure is repeated for each output y_i, thus, there will be a set of m equations

given by:

$$\begin{bmatrix} y_1^{(r_1)} \\ \vdots \\ y_m^{(r_m)} \end{bmatrix} = \begin{bmatrix} L_f^{r_1} h_1(x) \\ \vdots \\ L_f^{r_m} h_m(x) \end{bmatrix} + \Delta(x) = \begin{bmatrix} u_1 \\ \vdots \\ u_m \end{bmatrix} \tag{A.39}$$

Where $\Delta(x)$ is expressed by:

$$\Delta(x) = \begin{bmatrix} L_{g1} L_f^{r_1-1} h_1 & \cdots & L_{gm} L_f^{r_1-1} h_1 \\ \vdots & \vdots & \vdots \\ L_{g1} L_f^{r_m-1} h_m & \cdots & L_{gm} L_f^{r_m-1} h_1 \end{bmatrix} \tag{A.40}$$

$\Delta(x)$ is suitably called as the decoupling matrix for the MIMO system. If $\Delta(x)$ nonsingular, then the control u can be obtained as:

$$u = -\Delta^{-1}(x) \begin{bmatrix} L_f^{r_1} h_1(x) \\ \vdots \\ L_f^{r_m} h_m(x) \end{bmatrix} + \Delta^{-1}(x) \begin{bmatrix} v_1 \\ \vdots \\ v_2 \end{bmatrix} \tag{A.41}$$

Where $v = [v_1, \ldots v_m]^T$ are the new set of inputs defined by the designer. The resultant dynamics of the system with new control is easily obtained by substitution of (A.41) into (A.39) and is given by

$$\begin{bmatrix} y_1^{(r_1)} \\ \vdots \\ y_m^{(r_m)} \end{bmatrix} = \begin{bmatrix} v_1 \\ \vdots \\ v_2 \end{bmatrix} \tag{A.42}$$

It is readily noticed that the input–output relation in (A.42) is decoupled and linear.

Lazhar Manaï was born in Tunis, Tunisia on November 25, 1971, He received the mastery degree in Electrical engineering from Normal higher school of technical education, Tunis-Tunisia (ENSET: Ecole Normale Supérieure de l'Enseignement Technique) in 1997, and (DEA) and the PHD degree from ENIT, in 2003 and 2008 respectively.

He is interested in the power electronics and machine modelling control induction Motor drives, Pulse Width Modulation, Multilevel inverter and active filter.

Dr. Lazhar occupied from 1997 to 2001 the post of teacher of technology in secondary education. Since 2003 he's assistant professor in higher institute of industrial systems of Gabes

Faouzi Ben Ammar was born in Tunis, Tunisia on May 15, 1962 . He received the Engineer degree in Electrical engineering from National Engineering School of Monastir-Tunisia (Ecole Nationale d'Ingénieurs de Monastir ENIM), in 1987, and (DEA) and the PHD degree from the National polytechnic Institute of Toulouse, France (INPT ENSEEIHT) in 1989 and 1993 respectively.

He is interested in the power electronics and machine modelling control induction Motor drives, Pulse Width Modulation, Multilevel inverter, active filter, Reliability.

Dr. Faouzi occupied From 1993 to 1998 engineer's post in Alstom company in France–Belfort in the development of control drives systems. He joined the National Institute of Applied sciences and Technology of Tunis (Institut National des Sciences Appliquées et de Technologie de Tunis) in 1998 as assistant professor. Since 2004 he has been HDR and professor of power electronics at the same Institute.